AMERICAN SOCIETY FOR MICROBIOLOGY | Antimicrobial Agents and Chemotherapy

Biofilms of Pathogenic Nontuberculous Mycobacteria Targeted by New Therapeutic Approaches

Thet Tun Aung,[a,b] Joey Kuok Hoong Yam,[c] Shuimu Lin,[a] Shuhaida Mohamed Salleh,[a] Michael Givskov,[c] Shouping Liu,[a,d] Nyein Chan Lwin,[a] Liang Yang,[b,c] Roger W. Beuerman[a,d,e]

Singapore Eye Research Institute, Singapore[a]; School of Biological Sciences, Nanyang Technological University, Singapore[b]; Singapore Centre on Environmental Life Sciences Engineering (SCELSE), Nanyang Technological University, Singapore[c]; SRP Neuroscience and Behavioral Disorders, Duke-NUS, Singapore[d]; Department of Ophthalmology, Yong Loo Lin School of Medicine, National University of Singapore, Singapore[e]

Microbial infections of the cornea are potentially devastating and can result in permanent visual loss or require vision-rescuing surgery. In recent years, there has been an increasing number of reports on nontuberculous mycobacterial infections of the cornea. Challenges to the management of nontuberculous mycobacterial keratitis include delayed laboratory detection, low index of clinical suspicion, poor drug penetration, slow response to therapy, and prolonged use of antibiotic combinations. The ability of nontuberculous mycobacteria to evade the host immune response and the ability to adhere and to form biofilms on biological and synthetic substrates contribute to the issue. Therefore, there is an urgent need for new antimicrobial compounds that can overcome these problems. In this study, we evaluated the biofilm architectures for *Mycobacterium chelonae* and *Mycobacterium fortuitum* in dynamic flow cell chamber and 8-well chamber slide models. Our results showed that mycobacterial biofilms were quite resistant to conventional antibiotics. However, DNase treatment could be used to overcome biofilm resistance. Moreover, we successfully evaluated a new antimicrobial compound (AM-228) that was effective not only for planktonic mycobacterial cells but also for biofilm treatment and was compared favorably with the most successful "fourth-generation" fluoroquinolone, gatifloxacin. Finally, a new treatment strategy emerged: a combination of DNase with an antibiotic was more effective than an antibiotic alone.

Keratitis, inflammation of the cornea of the eye, is often due to an infection by either bacteria or fungi. Effective antibiotic treatment can require considerable time, increasing the risk to vision and the need for sight-restoring surgery. Common risk factors for infectious keratitis include ocular trauma, contact lens wear, recent ocular surgery, preexisting ocular surface disease, dry eye, lid deformity, impairment of corneal sensation, chronic use of topical steroids, and systemic immunosuppression (1–4). Bacterial keratitis is one of the most important causes of corneal opacification, which is the second most common cause of legal blindness worldwide, after cataracts (5). In Minnesota, the incidence of ulcerative keratitis was found to increase 435% from the 1950s to the 1980s (6). Since Runyon classified mycobacteria in 1959 (7), nontuberculous mycobacteria (NTM) have become increasingly recognized as an important cause of ocular morbidity (8). NTM can cause periocular, cutaneous, adnexal, orbital (9–11), conjunctival (12, 13), scleral (12, 14), and corneal (15–17) infections. Among NTM isolates, the most prevalent pathogenic strains for the eye are *Mycobacterium chelonae* and *Mycobacterium fortuitum* (18–20). One study found that among 183 NTM clinical isolates from an ophthalmology clinic, keratitis comprised (36.6%) of the cases, which was the most common pathogenesis, followed by scleral buckle infections (14.8%) and socket and implant infections (14.8%) (18). There were several reports showing that NTM keratitis developed following refractive surgery (21, 22).

Biofilms are communities of bacteria adhering to the tissue surface and to each other by producing an extracellular polysaccharide matrix often called slime. It has been suggested that 80% of all bacterial infections have a biofilm stage, and recent studies have emphasized biofilm involvement in eye infections (23, 24). The biofilm matrix is mainly composed of extracellular DNA, proteins, and polysaccharides. Bacteria can adhere to biotic or abiotic surfaces, where they communicate by forming single-species or multispecies colonies. Other factors may also contribute to biofilms in mycobacteria, such as the long-chain myclic acid lipids (25, 26). Glycopeptidolipids coat the cell wall and have been suggested to be important for attaching the mycobacterial biofilm to surfaces (27). Biofilm research in recent decades has shown that biofilms are complex and dynamic communities with substantial phenotypic diversification allowing microorganisms to adapt to diverse environments (28–34).

It is generally accepted that the presence of a biofilm is associated with increased antibiotic resistance. *Mycobacterium fortuitum* and *Mycobacterium chelonae* biofilms have been found under various conditions of both low and high nutrient contents (35). In this study, we successfully monitored the biofilm architecture developed by *M. chelonae and M. fortuitum* in a dynamic flow cell model and in an 8-well chamber slide model. We identified a new

Received 1 July 2015 **Returned for modification** 20 July 2015
Accepted 21 September 2015

Accepted manuscript posted online 12 October 2015

Citation Aung TT, Yam JKH, Lin S, Salleh SM, Givskov M, Liu S, Lwin NC, Yang L, Beuerman RW. 2016. Biofilms of pathogenic nontuberculous mycobacteria targeted by new therapeutic approaches. Antimicrob Agents Chemother 60:24–35. doi:10.1128/AAC.01509-15.

Address correspondence to Liang Yang, yangliang@ntu.edu.sg, or Roger W. Beuerman, rwbeuerman@gmail.com.

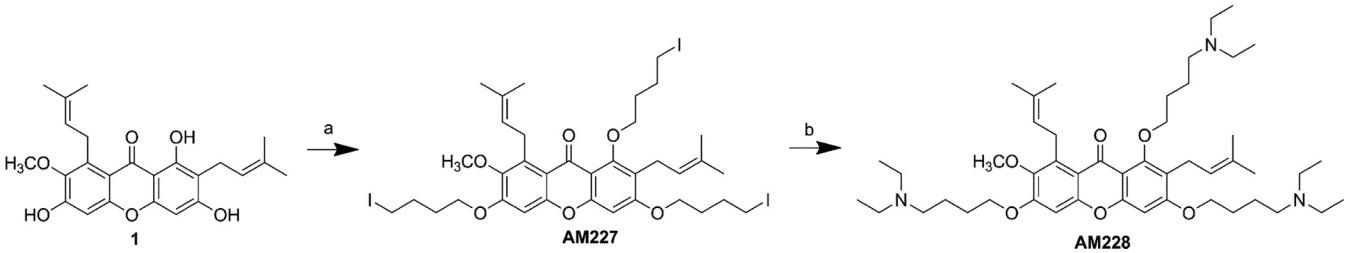

FIG 1 General synthetic routes for AM228. Reaction conditions were as follows: for route a, $I(CH_2)_4I$, K_2CO_3, acetone, reflux, 24 h, and 62% yield percentage, and for route b, diethylamine, DMSO, room temperature, 4 h, and 34% yield percentage.

antimicrobial compound, AM-228, which had outstanding antimicrobial properties against NTM in both planktonic and biofilm modes. Moreover, we proposed a new treatment strategy, a combination of DNase and antibiotic, which outperformed an antibiotic alone.

MATERIALS AND METHODS

Bacterial strains. *M. chelonae* ATCC 35752 and *M. fortuitum* (*M. neworleansense*) ATCC 49404 were used in this study. Bacteria were grown in Middlebrook broth containing 0.05% Tween 80 supplemented with albumin-dextrose-catalase (ADC) enrichment medium with shaking at 35°C. The liquid cultures were incubated for 3 to 5 days to obtain the desired growth.

Growth testing of suitable media for biofilm work. Growth testing in different media (Luria broth [LB], tryptic soy broth, Middlebrook broth, and minimal 63 medium) was carried out for 7 days. The liquid cultures were adjusted to an optical density at 600 nm (OD_{600}) of 0.05 in different media prior to the experiments. The cultures were incubated at 35°C in a rotary shaker (200 rpm). All media were supplemented with 0.05% Tween 80 to prevent cell clumping. An aliquot of the culture was taken out to check the growth with a spectrometer, and OD_{600} was determined at 12, 24, 48, 72, 96, and 120 h.

Establishment of flow cell system for nontuberculous mycobacteria. Mycobacterial biofilms were cultivated in flow chambers of three channels with dimensions of 40 mm by 4 mm by 1 mm. The flow chamber was set up as previously described (36) using Luria broth medium at 35°C. A diluted culture of 500 μl of *M. fortuitum* or *M. chelonae* at an OD_{600} of 0.1 was inoculated into each flow cell chamber. The flow cells were inverted without flow for 2 h after inoculation. Then the flow cells were changed back to an upright position, medium was fed into the flow cells using a Watson Marlow 205s peristaltic pump at a flow rate of 7.7 ml h^{-1}, and the cells were incubated at 35°C for 10 days. Luria broth containing Syto-9 (green fluorescence) from a LIVE/DEAD BacLight kit (L-7007; Molecular Probes) was added into each channel and viewed with a Zeiss LSM780 confocal laser scanning microscope (CLSM; Carl Zeiss, Jena, Germany) at an excitation wavelength of 480 nm and an emission wavelength of 500 nm. CLSM images were taken at days 3, 5, 7, and 10.

Establishment of the 8-well chamber slide model for nontuberculous mycobacteria (high-throughput screening). Mycobacteria were cultivated in a μ-Slide 8-well glass bottom chamber slide (ibidi, Germany) for high-throughput biofilm analysis to screen antimicrobial compounds. Mid-log growth cultures were determined at an OD_{600} of 0.1 in Luria broth medium prior to inoculations. Two hundred microliters of the culture was placed into each well of an 8-well chamber slide and incubated at 35°C for 5 days (37). Fresh prewarmed medium was added along the wall of each chamber every 24 h without disrupting the biofilm. At each time point, medium was removed from the well and the resident biofilm was washed gently, twice, with sterile phosphate-buffered saline (PBS). Syto-9 (green fluorescence) from a LIVE/DEAD BacLight kit (L-7007; Molecular Probes) was added into each well and viewed with Zeiss LSM780 confocal laser scanning microscope (Carl Zeiss, Jena, Germany) at an excitation wavelength of 480 nm and an emission wavelength of 500 nm, and images were taken at days 1, 3, and 5.

General procedure for synthesis of AM-228. α-Mangostin (500 mg, 1.22 mmol) was dissolved in 10 ml of acetone. Potassium carbonate (7.5 eq) and 1,4-diiodobutane (15.0 eq) were added. The reaction mixture was refluxed for 24 h. After the reaction was complete, the solvent was removed under reduced pressure. The oil residue was diluted with ethyl acetate (EtOAc) and washed twice with saturated brine and once with water. The organic phase was dried over anhydrous Na_2SO_4 and then purified via silica gel column chromatography (petroleum ether-EtOAc, 15/1, vol/vol) to obtain intermediate AM-227.

Then, to a solution of AM-227 (100 mg, 0.11 mmol) in dimethyl sulfoxide (DMSO; 4 ml), diethylamine (4 ml) was added. The mixture was stirred at room temperature for 4 h. After completion of the reaction, the mixture was diluted with 50 ml of ethyl acetate and then washed with aqueous $NaHCO_3$ and saturated brine (each three times). The organic phase was dried over anhydrous Na_2SO_4 and concentrated under vacuum. The residual crude oil was purified via silica gel column chromatography (EtOAc-MeOH-Et_3N, 100/2/1, vol/vol) to afford AM-228. The general synthetic route of AM-228 is shown in Fig. 1.

Hemolytic activity. Potential drug toxicity was carried out using a hemolysis assay with fresh rabbit red blood cells (RBCs) for AM-228. The study was done under a protocol approved by the SingHealth IACUC and was in accordance with guidelines for animal research of the Association for the Research in Vision and Ophthalmology. Freshly isolated rabbit red blood cells were centrifuged at 3,000 rpm for 10 min and thoroughly washed with sterile PBS twice. The compound was mixed with RBCs to obtain the desired concentration (final vol/vol of RBCs = 45) and incubated at 37°C for 1 h in a 96-well plate (SPL Life Science). One hundred microliters of supernatant was transferred for measuring absorbance (576 nm) with a Tecan infinite 200-microplate reader. Triton X-100 (2%) was set up as a positive control, and PBS and *N*,*N*-dimethylformamide (DMF) (1%) were used as a negative control. The following equation was used to calculate the percentage of hemolysis: percent hemolysis = (mixture A_{576} − negative-control A_{576})/(positive-control A_{576} − negative-control A_{576}) ×100 (38).

Chemical toxicity testing using rabbit corneal wound healing model. Six New Zealand rabbits were purchased from the National University of Singapore. All animal experiments were conducted in compliance with the ARVO statement for the use of animals in ophthalmic and vision research and the *Guide for the Care and Use of Laboratory Animals* (39) and under the supervision of the SingHealth Experimental Medical Centre (SEMC). Ethics approval was obtained from SingHealth IACUC. Six New Zealand White rabbits were assigned randomly into two groups, a control group treated with PBS and a group treated with AM-228 at 3 mg/ml. Rabbits were anesthetized, and corneas received 1% xylocaine. A corneal wound was made by using a 5-mm trephine, and mechanical removal of epithelial cells was carried out by sterile miniblade (BD-Beaver), leaving the basal lamina intact (40). Topical application of the respective drug was done 3 times/day. The cornea wound was visualized every day until closure by the aid of cobalt-blue filter-equipped slit lamp biomicroscopy, with staining with Minims fluorescein sodium eye drops,

which are routinely used in the ophthalmology clinic to check cornea damage. Fluorescein-stained images were analyzed for wound area by ImageJ. The results showed that AM-228 at 3 mg/ml did not delay wound healing compared with the control, PBS.

Determination of antimicrobial activity. Susceptibility testing for all compounds was performed in Luria broth (LB), since it did not show any MIC change from Middlebrook broth with ADC supplement (data not shown), and biofilm experiments used Luria broth. The broth microdilution method in accord with the NCCLS guidelines, with minor modifications, was followed (41). To determine the MIC, broth microdilution was used with LB containing 0.05% Tween 80. Briefly, AM-228 was dissolved in DMF to make 1,000-μg/ml stock solutions. Thereafter, LB was used to prepare serial 2-fold dilutions of the compound in the wells. The cultured suspensions were prepared in sterile PBS to a density of 0.5 MacFarland standard (OD_{600} = 0.1). One hundred microliters of this culture suspension was transferred into 15 ml of LB to make approximately 10^6 CFU/ml. The bacterial suspension (100 μl) in LB was transferred to each well with the compound to be tested. After inoculation, each well contained approximately 5×10^5 CFU/ml. The dilutions were tested in duplicate. Bacteria were incubated with the compounds for 5 days at 35°C prior to reading with a Tecan Infinite 200 microplate reader. The MIC was obtained by measuring the OD_{600} and visible growth (42, 43).

Time-kill kinetics. The culture was suspended and adjusted in LB to obtain a bacterial suspension with 10^5 to 10^6 CFU/ml. Then, the inoculum was treated with various concentrations of gatifloxacin or AM-228 in LB containing 0.05% Tween 80 and incubated at 35°C. Culture aliquots were removed at 6 h and on days 1, 2, 3, 4, and 5 for viable plate counts. The aliquots were serially diluted 10-fold, plated on LB agar plates, and incubated at 35°C for 3 to 5 days. Cell viability was determined by enumerating colonies growing on the plates. Bactericidal activity was defined as a 3-log reduction of viable counts in culture treated with the antimicrobial compound compared with that of the untreated control at a specific time point.

Biofilm treatment using AM-228 or gatifloxacin (8-well chamber slide biofilm model). *M. fortuitum* and *M. chelonae* were grown in an 8-well chamber slide as detailed above. The optimal DNase concentration that led to a significant reduction of biomass was determined by serial 2-fold dilutions of DNase I RQ1 RNase-Free DNase (M6101; Promega) using Luria broth. To evaluate the effects of antibiotic alone and in combination with DNase on NTM biofilm, AM-228 and gatifloxicin at 10× MIC individually as well as AM-228 at 10× MIC with DNase at an optimal concentration were diluted in LB. All the above-listed respective compounds were added to day 4 mycobacterial biofilms. The medium was untouched in the control well, and 24-h treatment of each compound was carried out.

(i) LIVE/DEAD cell imaging. At the end of the experiment, the medium was aspirated and Luria broth containing Syto-9 (green fluorescence) and 20 μM propidium iodide (PI) from a LIVE/DEAD BacLight kit (Molecular Probes) was dispensed into the antimicrobial-treated wells and control wells. For DNase experiments, wells with DNase alone received Luria broth containing Syto-9 and wells containing antibiotic and DNase received Luria broth containing Syto-9 and 20 μM PI from a LIVE/DEAD BacLight kit (Molecular Probes) to stain the biofilm. Stained cells were observed under CLSM using an argon laser (excitation wavelength of 480 nm and emission wavelength of 500 nm) and helium laser (excitation wavelength of 490 nm and emission wavelength of 635 nm), respectively. Confocal images were analyzed using IMARIS to obtain the live/dead ratios of the cells in antibiotic-treated wells and live biovolume in the DNase-treated wells. Three independent experiments were carried out, and five images were taken from each experiment for analysis. In brief, three-dimensional (3D) biofilm images were reconstructed using Surpass mode by IMARIS software. Surfaces were created for each channel, Syto-9 (green fluorescence) and propidium iodide (red fluorescence), in order to generate the biovolume. Finally, the average of the total biovolumes was exported and used for further analysis (44, 45). Statistical analysis used nonparametric tests (Kruskal-Wallis test and Mann-Whitney U test) and *post hoc* pairwise comparison employed by using PASW statistic 18. *P* values of ≤0.05 were considered statistically significant.

(ii) CFU measurement. At the end of experiment, the medium was aspirated and wells were washed thoroughly with PBS. Sterile 3-mm glass beads were used to disperse the biofilms. The aliquots were serially diluted 10-fold, plated on LB agar plates, and incubated at 35°C for 3 to 5 days. Cell viability was determined by enumerating colonies growing on the plates. The experiments were done in triplicate, and the results are shown as means ± standard deviations (SDs). Nonparametric testing (Mann-Whitney U test) was performed by using PASW statistic 18. *P* values of ≤0.05 were considered to be statistically significant.

RESULTS

Establishment of biofilm architectures in dynamic flow cell model and 8-well chamber slide model. Biofilms are bacterial communities embedded within a secreted matrix of extracellular polymeric substance (EPS). Initiation of a biofilm through attachment followed by microcolony formation and subsequent formation of heterogeneous biofilm communities are the initial steps to form a mature biofilm. These bacterial communities develop biomass, which conveys an extra measure or therapeutic resistance to an infection (46). Thus, we examined the *in vitro* biofilm forming potential and architecture using the dynamic flow cell biofilm model and 8-well chamber slide biofilm model. Mycobacteria were tested in different media in order to choose a suitable medium for biofilm experiments. The experiments indicated that growth was better in Middlebrook medium followed by tryptic soy broth and Luria broth (data not shown). However, *M. fortuitum* and *M. chelonae* formed thicker biofilms in Luria broth than in Middlebrook and minimal media (data not shown). Our results showed that *M. fortuitum* formed a biofilm earlier (day 1) than *M. chelonae* (day 3) in Luria broth (Fig. 2 and 3). Multiple finger-like projections and greater biofilm mass were observed in *M. fortuitum* biofilms (Fig. 2), while irregular diffuse colonies were formed in *M. chelonae* biofilms (Fig. 3). The results from 8-well chamber studies correlated with the flow cell model, and similar biofilms were observed in the 8-well chamber slide model for both mycobacteria (data not shown). Void areas were observed within mature biofilms of *M. fortuitum*.

Action of a new antimicrobial, AM-228, and biofilm resistance to antibiotic treatment. In clinical practice, the regimens to treat NTM infections of the cornea often require a combination of antibiotics applied for 2 to 3 months (20, 47). However, the slow therapeutic response complicated by poor drug penetration due to biofilm formation is an important barrier for treating NTM infections in the eye or skin. Therefore, new antimicrobial compounds which could eradicate infections of NTM more quickly would provide significant patient benefits. We have tested a new antimicrobial which was synthesized in our laboratory using a core molecule extracted from a natural compound found in a common Asian fruit, mangosteen. The results showed that AM-228 had good biocompatibility as demonstrated by the *in vitro* hemolysis assay (molecular weight, 792.1 g/mol; HC_{50} in testing with rabbit RBCs, >200 μg/ml) and *in vivo* rabbit corneal wound healing results (Fig. 4) and outstanding antimicrobial activity (Table 1). Time-kill studies revealed that AM-228 acted much more rapidly than the most active commercially available antibiotic, gatifloxacin. AM-228 essentially sterilized the *M. fortuitum* infection even when used at 1× MIC (Fig. 5). AM-228 and gatifloxacin showed a 3-log reduction in an

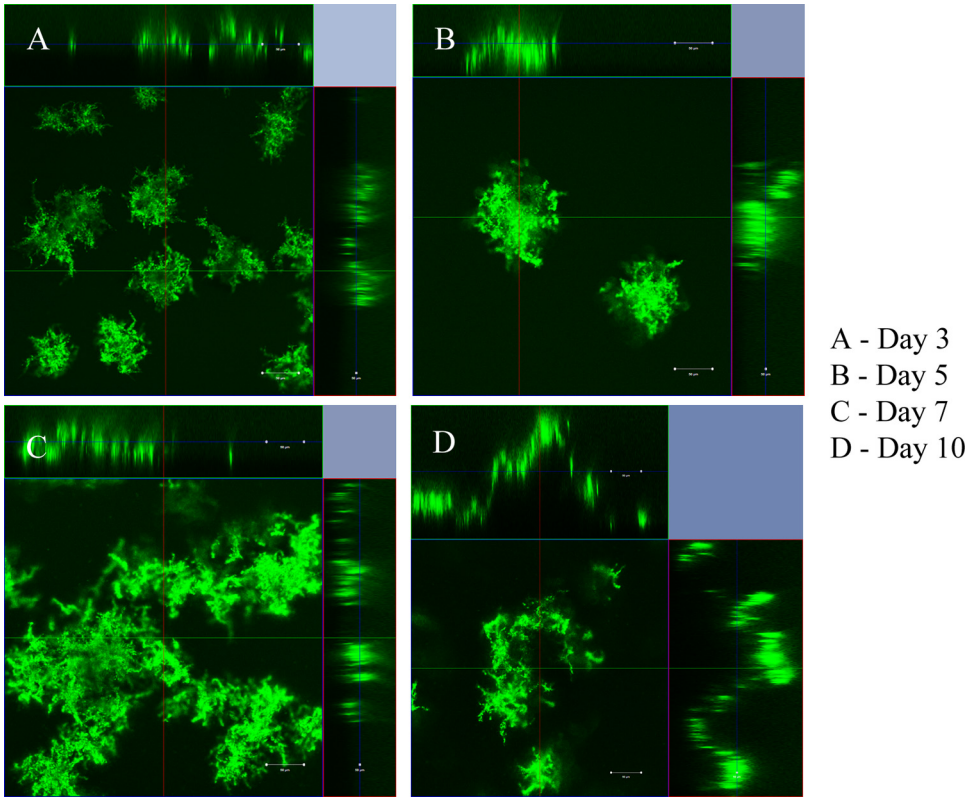

FIG 2 Formation of *M. fortuitum* biofilm in dynamic flow cell system. Finger-like projections from base of the structure formed as early as day 3. The biofilm mass increased as the days progressed, and the thickness was the greatest at day 10 (100 μm).

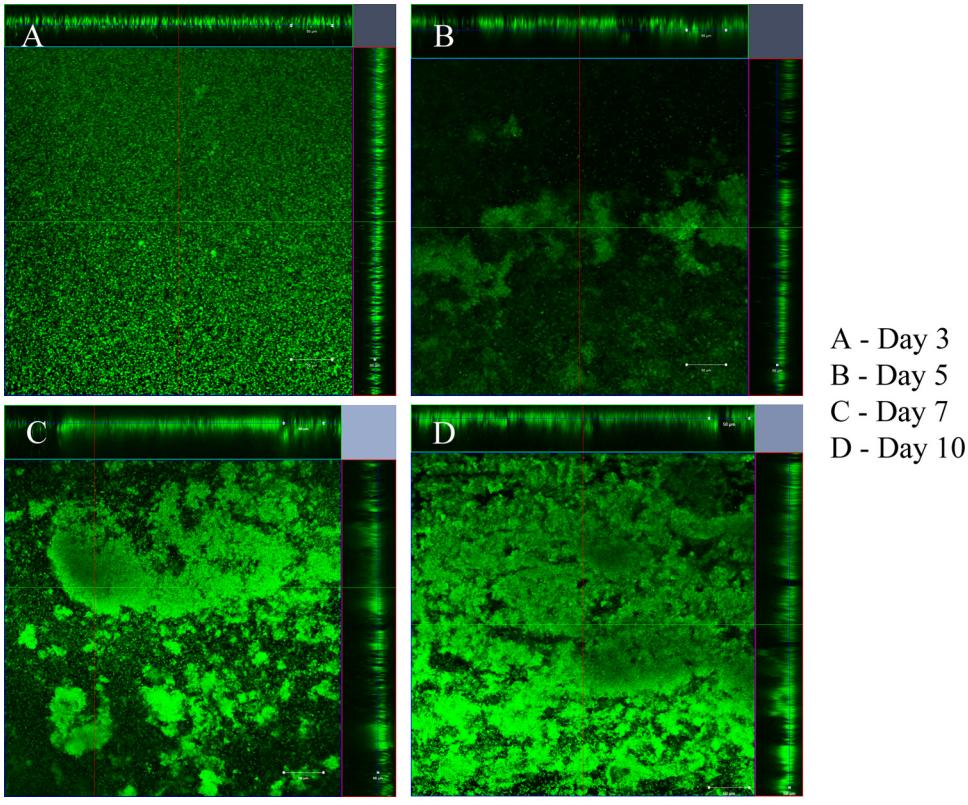

FIG 3 Formation of *M. chelonae* biofilm in the dynamic flow cell system. Biofilm formation started by day 5 as irregular short, flat structures in small microcolonies. Large diffuse microcolonies formed at days 7 and 10.

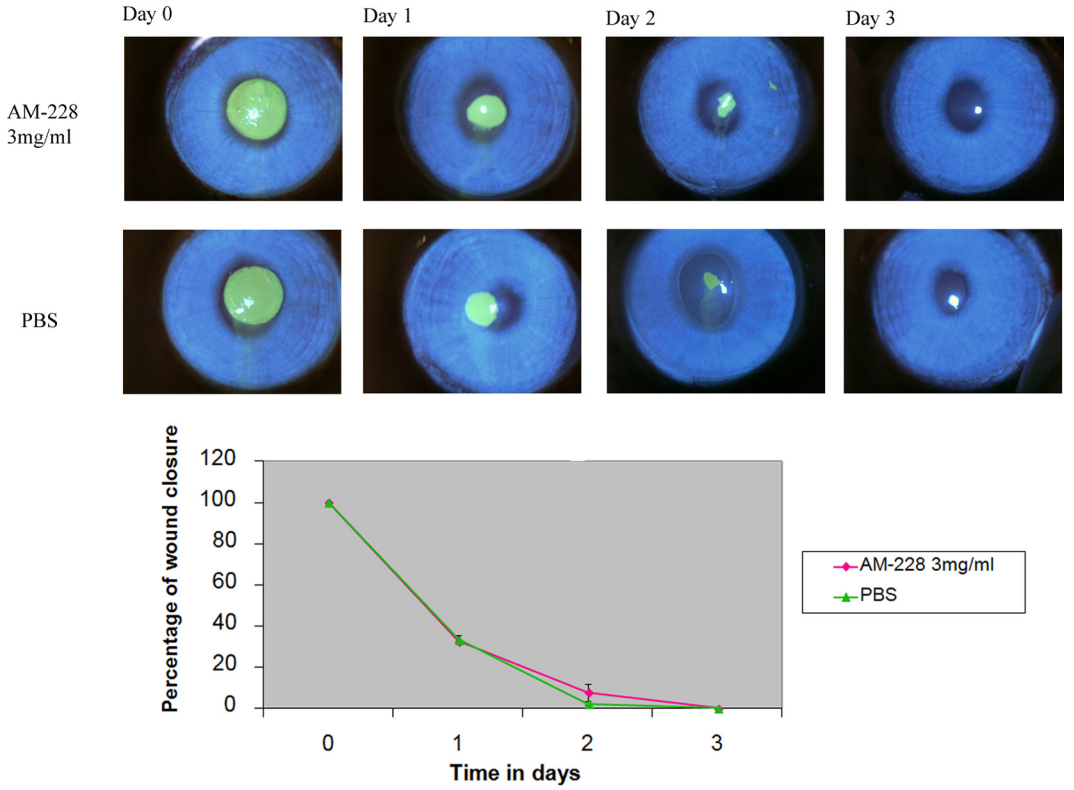

FIG 4 Chemical toxicity testing of AM-228 on corneal re-epithelialization in a rabbit wound healing model. Slit lamp images showed the normal wound healing pattern and rate compared with that of the control. There were no signs of inflammation or toxic effects on rabbit corneas treated with AM-228.

M. chelonae time-kill study after 48 h of treatment, but regrowth was seen with gatifloxacin treatment (Fig. 6).

It is generally acknowledged that bacteria in biofilms are resistant to antibiotic treatment, and nearly all bacterial infections have a biofilm component. We investigated the resistance of mycobacterial biofilms to antimicrobial compounds. It was found that mycobacterial biofilms were resistant to conventional antibiotics, such as gatifloxacin, while AM-228 was more active in killing biofilms formed by NTM in our study. AM-228 showed outstanding activity in terms of biovolume and CFU in treating both *M. fortuitum* biofilms (AM-228 versus control, $P = 0.003$ for biovolume and $P = 0.021$ for CFU; gatifloxacin versus control, $P = 0.019$ for biovolume and $P = 0.021$ for CFU) (Fig. 7) and *M. chelonae* biofilms (AM-228 versus control, $P = 0.004$ for biovolume and $P = 0.021$ for CFU; gatifloxacin versus control, $P = 0.005$ for biovolume and $P = 0.021$ for CFU) (Fig. 8).

DNase in mycobacterial biofilm treatment. Biofilm architecture is formed as a fibrous 3-dimensional network comprised of proteins, polysaccharides, lipids, and nucleic acids that act as a barrier for the penetration of antibiotics (48–50). Extracellular DNA (eDNA) has an important role in antibiotic resistance, and the destruction of eDNA was found to increase the efficacy of antibiotics (51). Moreover, eDNA plays a major role in horizontal gene transfer within the biofilm matrix, creating an opportunity for fast transmission of virulence factors and antibiotic resistance genes from one bacterial genome to another bacterial genome (52). The presence of eDNA in biofilm infections reduces chemokine production, prevents phagocytosis, and interferes with the innate immune response for the eradication of the infections (53). Therefore, the present study was designed to evaluate the role of eDNA in the treatment of NTM biofilms and to potentially develop a new treatment strategy, i.e., combining DNase and an antibiotic. An optimal DNase concentration that could maximally reduce the biomass was found (Fig. 9). Combination treatments (10× MIC of AM-228 plus optimal DNase concentration and 10× MIC of gatifloxacin plus optimal DNase concentration) for NTM biofilms were tested. The results showed that the combination treatments were more effective than the use of antibiotic alone to treat *M. fortuitum* biofilms (combination versus AM-228, $P = 0.018$ for biovolume and $P = 0.021$ for CFU; combination versus gatifloxacin, $P = 0.002$ for biovolume and $P = 0.043$ for CFU) (Fig. 10 and 11). For *M. chelonae* biofilm, the results were as follows: combination versus AM-228, $P = 0.006$ for biovolume and $P = 0.021$ for CFU; combination versus gatifloxacin, $P = 0.002$ for biovolume and $P = 0.021$ for CFU (Fig. 12 and 13).

TABLE 1 MICs of AM-228, gatifloxacin, amikacin, and tobramycin against *M. fortuitum* ATCC 49404 and *M. chelonae* ATCC 35752

	MIC (μg/ml) for:	
Antimicrobial	*Mycobacterium chelonae* ATCC 35752	*Mycobacterium fortuitum* ATCC 49404
AM-228	12.5	12.5
Gatifloxacin	0.195	0.195
Amikacin	25	3.125
Tobramycin	3.125	25

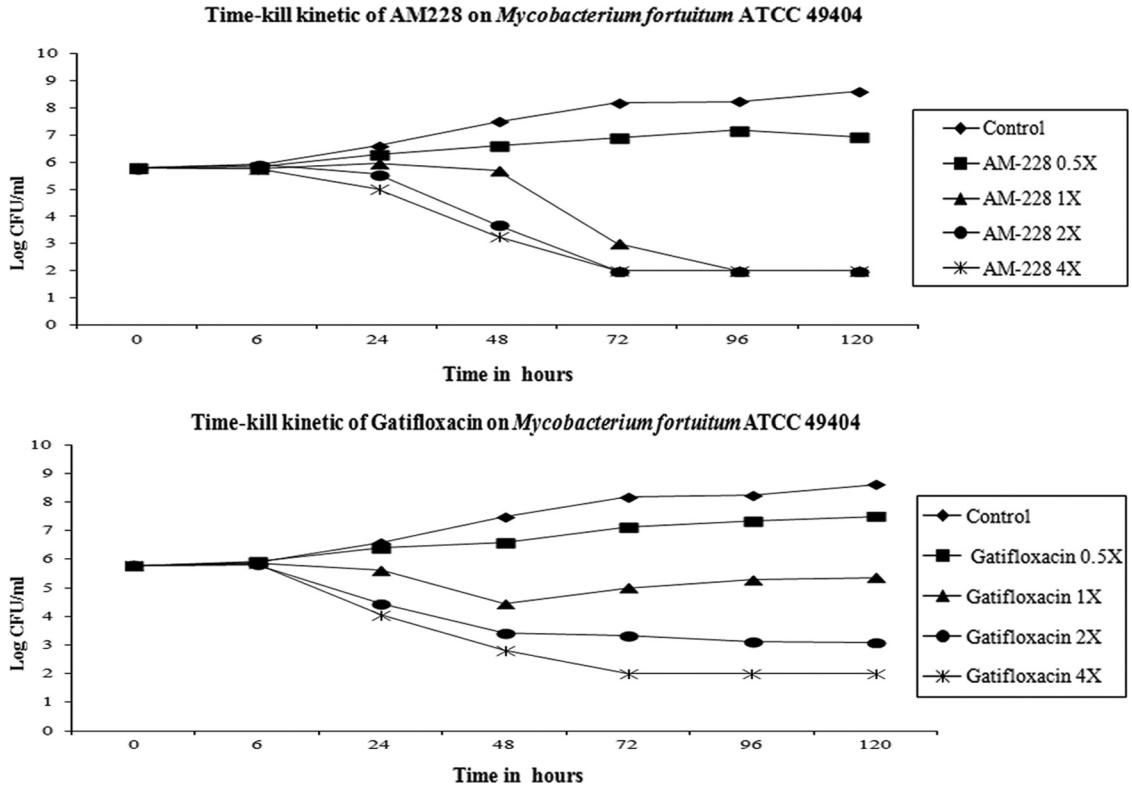

FIG 5 Time-kill curve of AM-228 and gatifloxacin on *M. fortuitum*. A 3-log reduction was seen at approximately 72 h after treatment with 1× MIC of AM-228, and the infection was sterile at 96 h after treatment. At 2× and 4× MIC, the solution was sterile at 72 h. Gatifloxacin treatment led to a 3-log reduction at approximately 48 h at 1× MIC. But at 2× and 4× MIC, the infection was not sterile until 120 h and 72 h after the treatment, respectively.

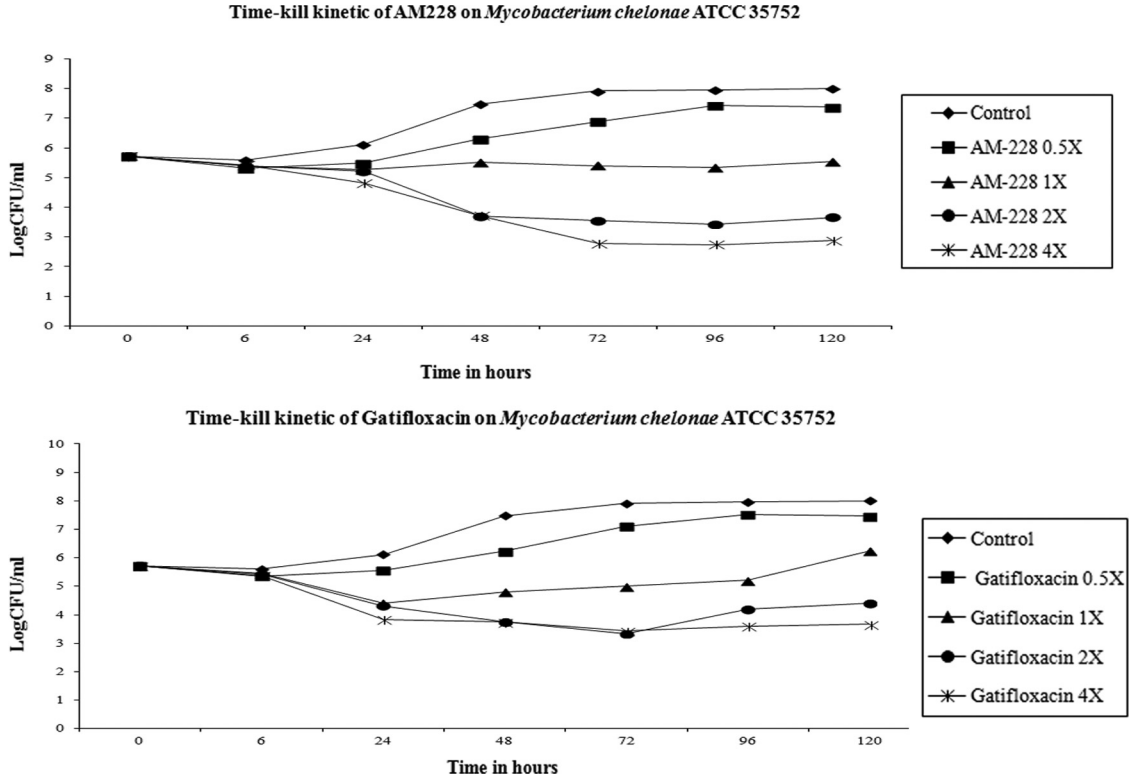

FIG 6 Time-kill curve of AM-228 and gatifloxacin on *M. chelonae*. A 3-log reduction was seen at 48 h after treatment with AM-228 at 2× MIC or 4× MIC. Gatifloxacin treatment at 2× MIC and 4× MIC provided a 3-log reduction at 48 h posttreatment. However, there was bacterial regrowth seen with 1× MIC and 2× MIC at 120 h after treatment.

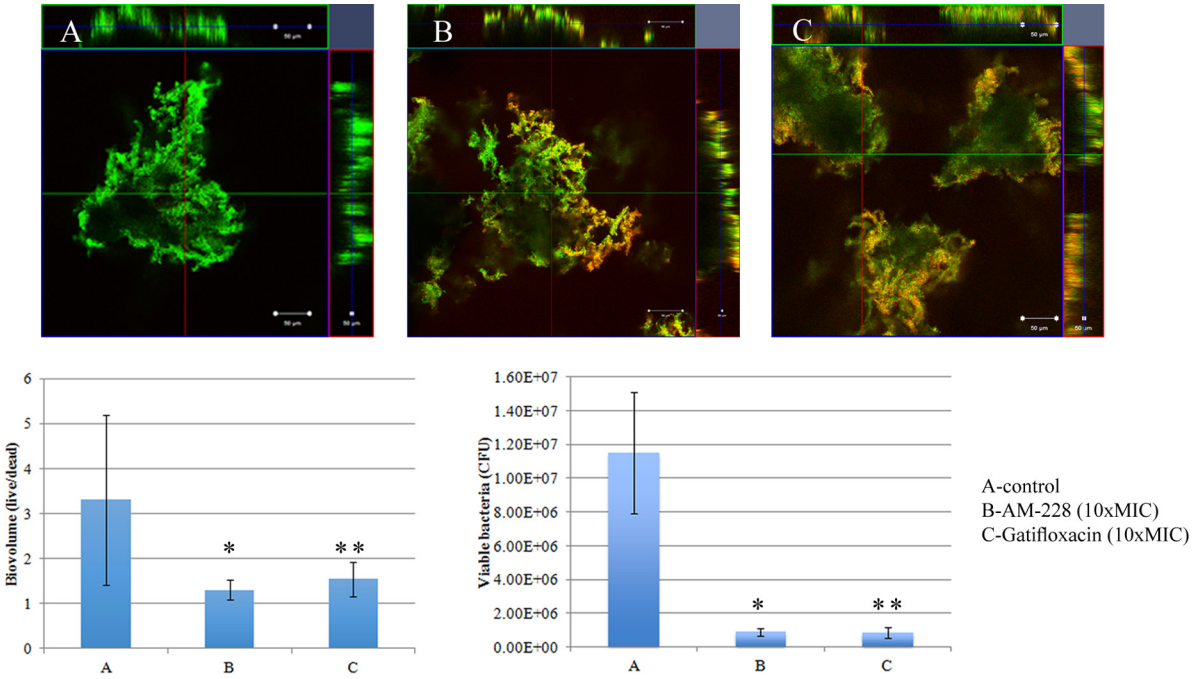

FIG 7 Confocal images of control *M. fortuitum* biofilm (day 5) (A) and *M. fortuitum* biofilm after treatment with AM-228 (B) or gatifloxicin (C) at 10× MIC. Green color represents live biomass, whereas red is dead biomass. Histograms show comparison of live/dead ratios and viable bacteria (CFU) after treatment of *M. fortuitum* biofilm. Scale bar, 50 μm. The values shown are means ± SDs from one representative experiment (five images); three independent experiments were done. Nonparametric tests (Kruskal-Wallis test and Mann-Whitney U test) and *post hoc* test (pairwise comparison) were employed using PASW statistic 18. AM-228 versus control, $P = 0.003$ for biovolume and $P = 0.021$ for CFU; gatifloxacin versus control, $P = 0.019$ for biovolume and $P = 0.021$ for CFU. * and **, $P \leq 0.05$ (considered to be statistically significant).

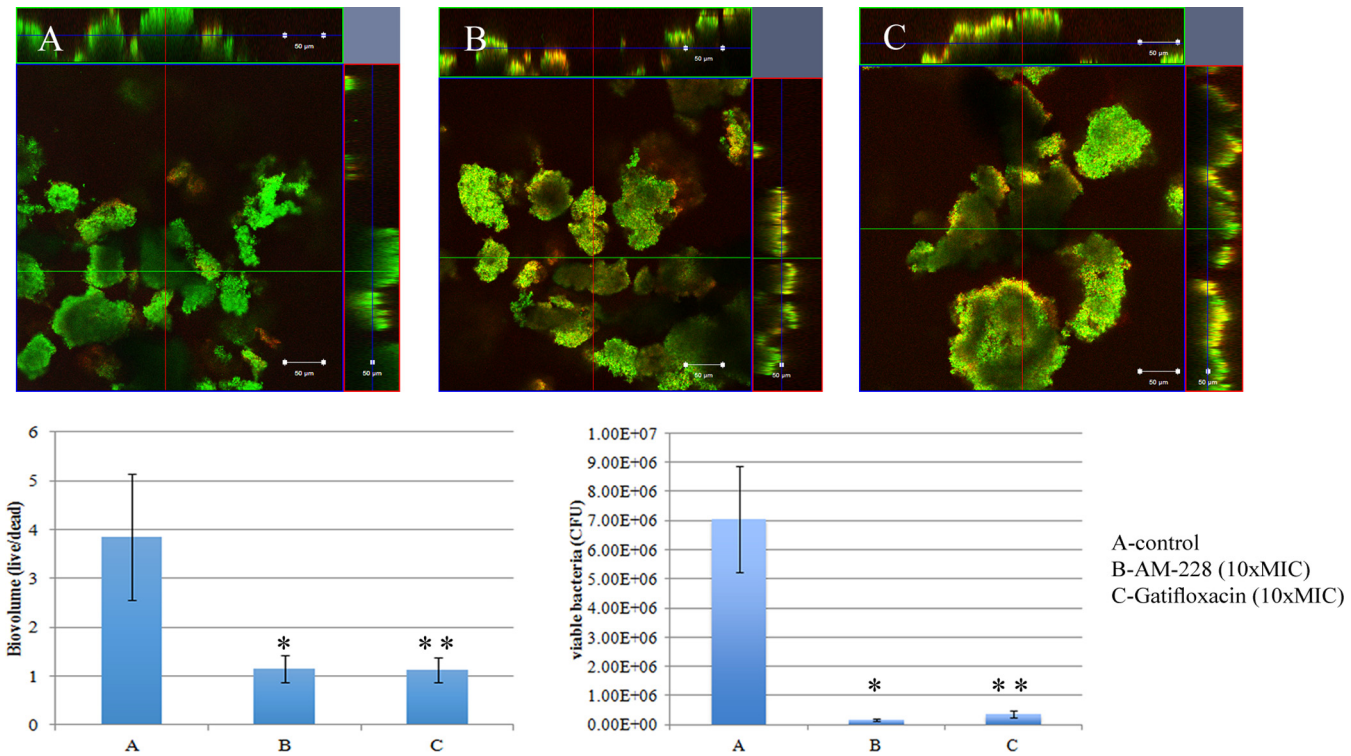

FIG 8 Confocal images of control *M. chelonae* biofilm (day 5) (A) and *M. chelonae* biofilm after treatment with AM-228 (B) or gatifloxicin (C) at 10× MIC. Green color represents live biomass, whereas red is dead biomass. Histograms show comparison of live/dead ratios and viable bacteria (CFU) after treatment of *M. chelonae* biofilm. Scale bar, 50 μm. The values shown are means ± SDs from one representative experiment (five images); three independent experiments were done. Nonparametric tests (Kruskal-Wallis test and Mann-Whitney U test) and *post hoc* test (pairwise comparison) were employed by using PASW statistic 18. AM-228 versus control, $P = 0.004$ for biovolume and $P = 0.021$ for CFU; gatifloxacin versus control, $P = 0.005$ for biovolume and $P = 0.021$ for CFU. * and **, $P \leq 0.05$ (statistically significant).

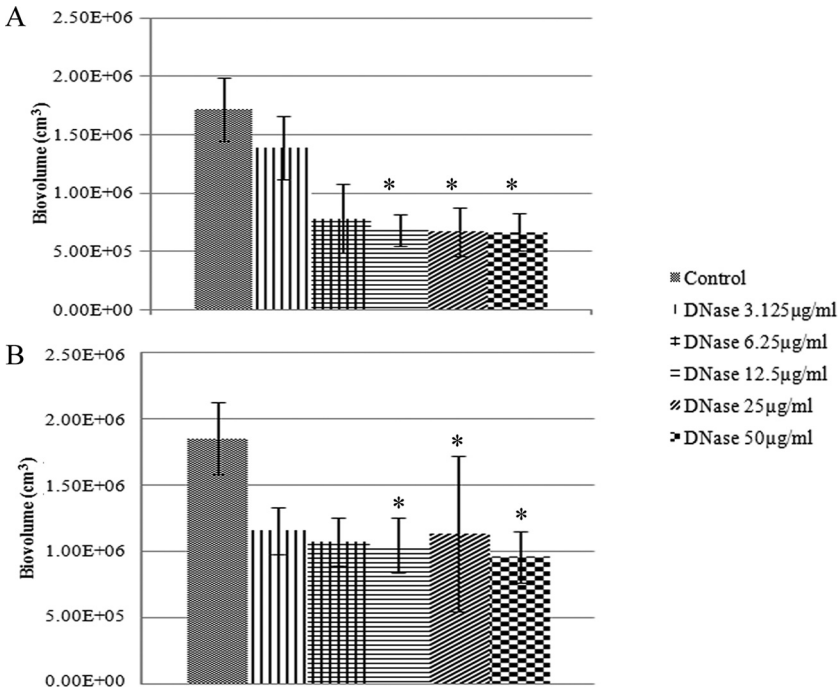

FIG 9 Response of *M. fortuitum* biofilm to DNase treatment (A) and response of *M. chelonae* biofilm to DNase treatment (B). Biovolume was compared following serial dilutions of DNase. The values shown are means ± SDs from one representative experiment (five images); three independent experiments were done. A nonparametric test (Kruskal-Wallis test) and *post hoc* test (pairwise comparison) were employed by using PASW statistic 18. There was a significant difference ($P \leq 0.05$) between groups (12.5, 25, and 50 μg/ml) when DNase was compared against the control for both strains. *, $P \leq 0.05$ (statistically significant).

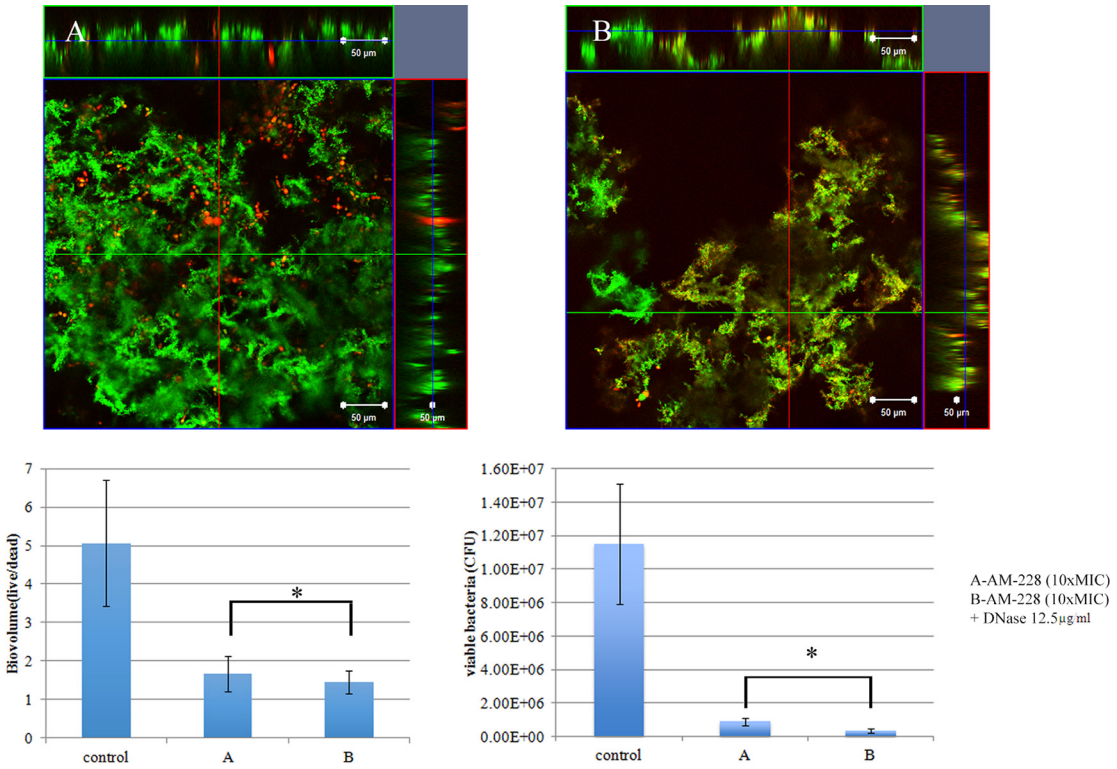

FIG 10 Combination treatment of AM-228 (10× MIC) and DNase (12.5 μg/ml) on *M. fortuitum* biofilm. Confocal images of *M. fortuitum* biofilm after treatment with AM-228 at 10× MIC (A) or AM-228 at 10× MIC and DNase at 12.5 μg/ml (B) are shown. Green color represents live biomass, whereas red is dead biomass. Histograms show comparison of live/dead ratios and viable bacteria (CFU) after treatment of *M. fortuitum* biofilm. Scale bar, 50 μm. The values are means ± SDs from one representative experiment (five images); three independent experiments were done. Combination treatment performed somewhat better than AM-228 alone. Live/dead ratios and CFU were compared using Mann-Whitney U test for the combination versus AM-228. $P = 0.018$ for biovolume, and $P = 0.021$ for CFU. *, $P \leq 0.05$ (statistically significant).

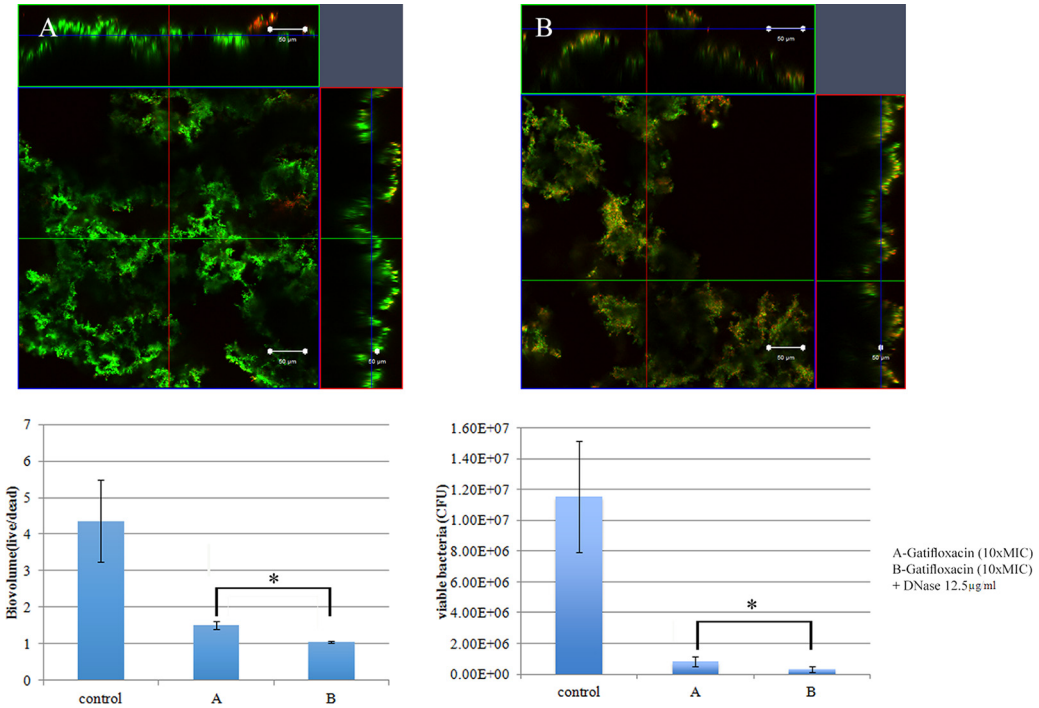

FIG 11 Combination treatment using gatifloxacin (10× MIC) and DNase (12.5 μg/ml) on *M. fortuitum* biofilm. Confocal images of *M. fortuitum* biofilm after treatment with gatifloxacin at 10× MIC (A) or gatifloxacin at 10× MIC and DNase at 12.5 μg/ml (B) are shown. Green color represents live biomass, whereas red is dead biomass. Histograms show comparison of live/dead ratios and viable bacteria (CFU) after treatment of *M. fortuitum* biofilm. Scale bar, 50 μm. The values are means ± SDs from one representative experiment (five images); three independent experiments were done. Combination treatment performed somewhat better than gatifloxacin alone. Live/dead ratios and CFU were compared by using Mann-Whitney U test between two different groups. Combination versus gatifloxacin, $P = 0.002$ for biovolume and $P = 0.043$ for CFU. *, $P \leq 0.05$ (statistically significant).

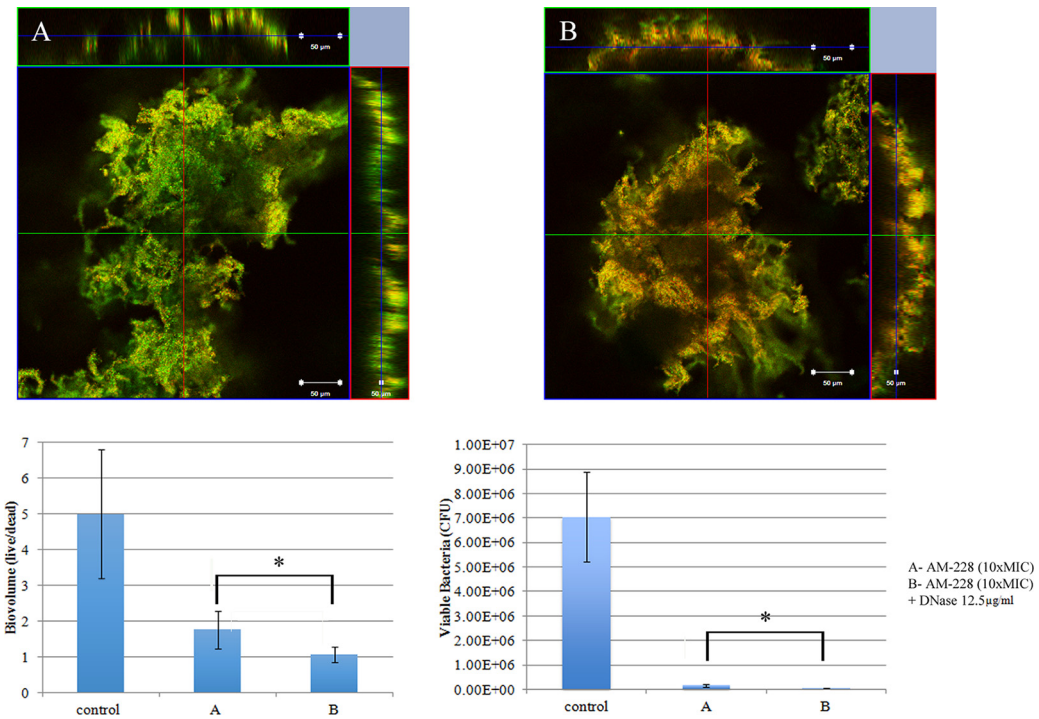

FIG 12 Combination treatment of AM-228 (10× MIC) and DNase (12.5 μg/ml) on *M. chelonae* biofilm. Confocal images of *M. chelonae* biofilm after treatment with AM-228 at 10× MIC (A) or AM-228 at 10× MIC and DNase at 12.5 μg/ml (B) are shown. Green color represents live biomass, whereas red is dead biomass. Histograms show comparison of live/dead ratios and viable bacteria (CFU) after treatment of *M. chelonae* biofilm. Scale bar, 50 μm. The values shown are means ± SDs from one representative experiment (five images); three independent experiments were done. Combination treatment was more efficient than AM-228 treatment. Live/dead ratios were compared using the Mann-Whitney U test between two different groups. Combination versus AM-228, $P = 0.006$ for biovolume and $P = 0.021$ for CFU. *, $P \leq 0.05$ (statistically significant).

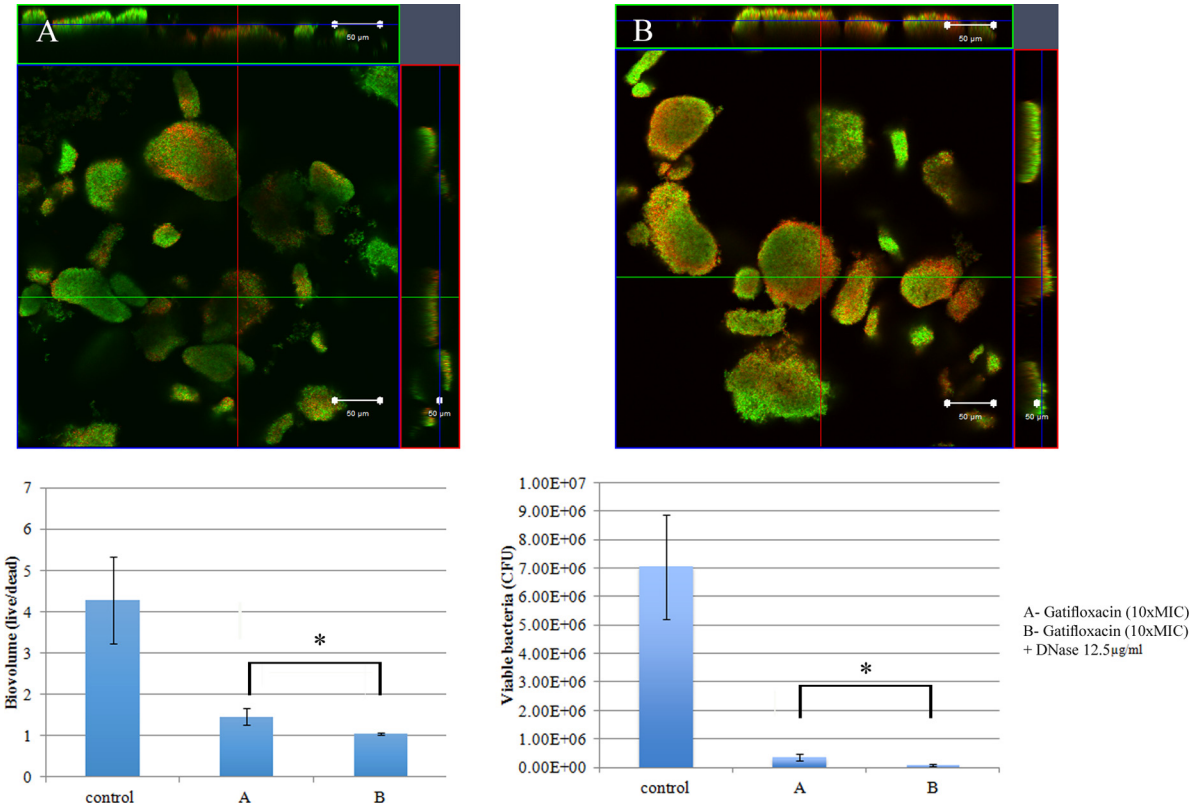

FIG 13 Combination treatment of Gatifloxacin (10× MIC) and DNase (12.5 μg/ml) on *M. chelonae* biofilm. Confocal images of *M. chelonae* biofilm after treatment with gatifloxacin at 10× MIC (A) or AM-228 at 10× MIC and DNase at 12.5 μg/ml (B) are shown. Green color represents live biomass, whereas red is dead biomass. Histograms show comparison of live/dead ratios and viable bacteria (CFU) after treatment of *M. chelonae* biofilm. Scale bar, 50 μm. The values shown are means ± SDs from one representative experiment (five images); three independent experiments were done. Combination treatment was more effective than individual treatment. Live/dead ratios and CFU were compared using the Mann-Whitney U test for the combination versus gatifloxacin ($P = 0.002$ for biovolume and $P = 0.021$ for CFU). *, $P \leq 0.05$ (statistically significant).

DISCUSSION

Nontuberculous mycobacteria (NTM), atypical mycobacteria, are nonmotile, non-spore-forming slender bacilli that are aerobic, opportunistic free-living pathogens found in the environment, including soil and water sources, food, dust, aerosols, and animals (54, 55). They have also been discovered in drinking water distribution systems and are relatively resistant to chlorine, organomercurials, and other routine disinfectants (54, 56, 57). Moreover, they possess the ability to form biofilms and survive under a wide range of temperature, pH, salinity, oxygen tension, and low-nutrient conditions (56, 58). Diagnosis of mycobacterium infection requires considerable time due to its slow growth, and patients may be misdiagnosed with infections with other bacteria, such as diphtheroids or *Nocardia* (59).

The average time required for the conclusive diagnosis of mycobacterial keratitis was around 4 months in postsurgical cases in south Florida (60). Nontuberculous mycobacterial infections in and around the eye are clinically recalcitrant to treatment, recur after cessation of therapy, and require long-term therapy (2 to 3 months) to eradicate (20, 47). The treatment of NTM infections is also complicated because identification and determination of *in vitro* antibiotic sensitivities can be delayed for weeks. These factors and a low index of clinical suspicion often result in inefficient treatment of NTM infections. Moreover, topical steroid usage prior to a correct diagnosis may worsen the prognosis (61). Amikacin was an early treatment of choice, but this drug has been shown to have poor penetration through an intact corneal epithelium (62). Another report showed that amikacin was not effective in NTM infections of the eye (61). Combination therapy with clarithromycin and amikacin for 3 to 4 months has been used for treating NTM infections (20, 47). Recent studies have suggested that the fluoroquinolones are useful for treating NTM infections (63). Reports on NTM resistance to ciprofloxacin and gatifloxacin have been published (64–66).

NTM infections are further complicated by the fact that bacterial biofilms play important roles in ocular infections (23). NTM growth in a biofilm is associated with numerous genetic and phenotypic differences because of their high hydrophobicity, with increased resistance to antibiotic therapy as the result (67). Mycobacteria can readily form biofilms and, because of their hydrophobicity and metal resistance, are among the earliest-known biofilm formers (67). In this study, we attempted to understand the treatment response of NTM biofilms. Different biofilm architectures for *M. chelonae* and *M. fortuitum* as well as the response to antimicrobial compounds were observed. We observed void areas within mature biofilms of *M. fortuitum*, which might result from production of biofilm-dispersing agents, such as biosurfactant. *M. chelonae* and *M. fortuitum* formed thick biofilms with irregular shapes that were relatively resistant to conventional antibiotics even at 10× MIC. Our data indicated that gatifloxacin, a "fourth-

generation" fluoroquinolone, is an effective antibiotic against NTM, corroborating clinical observations. However, our new antimicrobial AM-228 showed outstanding bacterial killing efficiency in time-kill studies and eradication of mycobacterial biofilms comparable to that with gatifloxacin. Bacteria within biofilms resist antibiotics more than planktonic bacteria not only because of limitation of antibiotic penetration but also because the biofilm matrix may inactivate antimicrobials (68). eDNA has been discovered in *Mycobacterium avium* biofilms, and combination treatment with DNase and antibiotic has been investigated (51). However, this is the first report showing the effectiveness of DNase treatment for *Mycobacterium fortuitum* and *M. chelonae* biofilms. In this study, DNase treatment of NTM biofilm reduced the biofilm biomass, suggesting that eDNA might be present with a role in the properties of the biofilm. Combination treatment with DNase (12.5 μg/ml) and 10× MIC of AM-228 or gatifloxacin clearly showed a significant eradication of bacteria in NTM biofilms, suggesting that destruction of eDNA by DNase leads to a decrease in the extracellular matrix, allowing better penetration and efficacy of AM-228 or gatifloxacin. However, future studies focusing on NTM biofilm matrix and the role of eDNA in NTM biofilm communities as well as studies of AM-228 in *in vivo* should be carried out in order to fill the gap of new drugs for NTM eye infections.

ACKNOWLEDGMENTS

We acknowledge the support of funding from NMRC/TCR/002-SERI/2012/R1018 and SHF/FG538P/2013 from the Ministry of Education of Singapore under its Research Centre of Excellence Programme and AcRF Tier 2 (MOE2014-T2-2-172) from the Ministry of Education, Singapore.

We declare no conflicts of interest.

FUNDING INFORMATION

Ministry of Health—Singapore (MOH) provided funding to Roger W. Beuerman and Shou Ping Liu under grant number NMRC/TCR/002-SERI/2012/R1018. Ministry of Health—Singapore (MOH) provided funding to Roger W. Beuerman and Shou Ping Liu under grant number SHF/FG538P/2013. Ministry of Education—Singapore (MOE) provided funding to Michael Givskov and Liang Yang under grant numbers Research Centre of Excellence Programme and AcRF Tier 2 (MOE2014-T2-2-172).

We appreciate the support of our funding agencies to make this research feasible.

REFERENCES

1. **Stapleton F, Edwards K, Keay L, Naduvilath T, Dart JK, Brian G, Holden B.** 2012. Risk factors for moderate and severe microbial keratitis in daily wear contact lens users. Ophthalmology **119:**1516–1521. http://dx.doi.org/10.1016/j.ophtha.2012.01.052.
2. **Ahn M, Yoon KC, Ryu SK, Cho NC, You IC.** 2011. Clinical aspects and prognosis of mixed microbial (bacterial and fungal) keratitis. Cornea **30:**409–413.
3. **Amescua G, Miller D, Alfonso EC.** 2012. What is causing corneal ulcer? Management strategies for unresponsive corneal ulceration. Eye **26:**28–36.
4. **Bharathi MJ, Ramakrishnan R, Meenakshi R, Shivakumar C, Lional Raj L.** 2009. Analysis of the risk factors predisposing to fungal, bacterial & Acanthamoeba keratitis in south India. Indian J Medical Res **130:**749–757.
5. **Bialasiewicz AA, Schonherr U, Schmitt T, Naumann GOH.** 1985. Triple therapeutic approach for keratitis, p 266. *In* Bialasiewicz AA, Schaal KP (ed), Infectious diseases of the eye. Aeolus Press, Buren, Netherlands.
6. **Erie JC, Nevitt MP, Hodge DO, Ballard DJ.** 1993. Incidence of ulcerative keratitis in a defined population from 1950 through 1988. Arch Ophthalmol **111:**1665–1671. http://dx.doi.org/10.1001/archopht.1993.01090120087027.
7. **Runyon EH.** 1959. Anonymous mycobacteria in pulmonary disease. Med Clin North Am **43:**273–290.
8. **Runyon EH.** 1970. Identification of mycobacterial pathogens using colony characteristics. Am J Clin Pathol **54:**578–586.
9. **Artenstein AW, Eiseman AS, Campbell GC.** 1993. Chronic dacryocystitis caused by Mycobacterium fortuitum. Ophthalmology **100:**666–668. http://dx.doi.org/10.1016/S0161-6420(93)31591-5.
10. **Chen SH, Wang CH, Chen HC, Weng GC, Lin PY, Wei FC.** 2001. Upper eyelid mycobacterial infection following Oriental blepharoplasty in a pulmonary tuberculosis patient. Aesthetic Plast Surg **25:**295–298. http://dx.doi.org/10.1007/s002660010141.
11. **Gonzalez-Fernandez F, Kaltreider SA.** 2001. Orbital lipogranulomatous inflammation harboring Mycobacterium abscesses. Ophthal Plast Reconstr Surg **17:**374–380. http://dx.doi.org/10.1097/00002341-200109000-00013.
12. **Margo CE, Pavan PR.** 2000. Mycobacterium chelonae conjunctivitis and scleritis following vitrectomy. Arch Ophthalmol **118:**1125–1128. http://dx.doi.org/10.1001/archopht.118.8.1125.
13. **Merani R, Orekondy S, Gottlieb T, Janarthanan P, McCarthy S, Karim R, Booth F.** 2008. Postoperative Mycobacterium abscessus nodular conjunctivitis. Clin Exp Ophthalmol **36:**371–373. http://dx.doi.org/10.1111/j.1442-9071.2008.01772.x.
14. **Hsiao CH, Chen JJ, Huang SC, Ma HK, Chen PY, Tsai RJ.** 1998. Intrascleral dissemination of infectious scleritis following pterygium excision. Br J Ophthalmol **82:**29–34. http://dx.doi.org/10.1136/bjo.82.1.29.
15. **Alvarenga L, Freitas D, Hofling-Lima AL, Belfort R, Jr, Sampaio J, Sousa L, Yu M, Mannis M.** 2002. Infectious post-LASIK crystalline keratopathy caused by nontuberculous mycobacteria. Cornea **21:**426–429. http://dx.doi.org/10.1097/00003226-200205000-00020.
16. **Brancato R, Carones F, Venturi E, Cavallero A, Gesu G.** 1997. Mycobacterium chelonae keratitis after excimer laser photorefractive keratectomy. Arch Ophthalmol **115:**1316–1318. http://dx.doi.org/10.1001/archopht.1997.01100160486019.
17. **Chandra NS, Torres MF, Winthrop KL, Bruckner DA, Heidemann DG, Calvet HM, Yakrus M, Mondino BJ, Holland GN.** 2001. Cluster of Mycobacterium chelonae keratitis cases following laser in-situ keratomileusis. Am J Ophthalmol **132:**819–830. http://dx.doi.org/10.1016/S0002-9394(01)01267-3.
18. **Girgis DO, Karp CL, Miller D.** 2012. Ocular infections caused by nontuberculous mycobacteria: update on epidemiology and management. Clin Exp Ophthalmol **40:**467–475. http://dx.doi.org/10.1111/j.1442-9071.2011.02679.x.
19. **Ford JG, Huang AJ, Pflugfelder SC, Alfonso EC, Forster RK, Miller D.** 1998. Nontuberculous mycobacterial keratitis in south Florida. Ophthalmology **105:**1652–1658. http://dx.doi.org/10.1016/S0161-6420(98)99034-0.
20. **Chang MA, Jain S, Azar DT.** 2004. Infections following laser in situ keratomileusis: an integration of the published literature. Surv Ophthalmol **49:**269–280. http://dx.doi.org/10.1016/j.survophthal.2004.02.007.
21. **Reviglio V, Rodriguez ML, Picotti GS, Paradello M, Luna JD, Juarez CP.** 1998. Mycobacterium chelonae keratitis following laser in situ keratomileusis. Refract Surg **14:**357–360.
22. **Solomon A, Karp CL, Miller D, Dubovy SR, Huang AJ, Culbertson WW.** 2001. Mycobacterium interface keratitis after laser in situ keratomileusis. Ophthalmology **108:**2201–2208. http://dx.doi.org/10.1016/S0161-6420(01)00851-X.
23. **Bispo PJM, Haas W, Gilmore MS.** 2015. Biofilms in infections of the eye. Pathogens **4:**111–136. http://dx.doi.org/10.3390/pathogens4010111.
24. **Saraswathi P, Beuerman RW.** 2015. Corneal biofilms: from planktonic to microcolony formation in an experimental keratitis infection with Pseudomonas aeruginosa. Ocul Surf **13:**331–345.
25. **Zambrano MM, Kolter R.** 2005. Mycobacterial biofilms: a greasy way to hold it together. Cell **123:**762–764. http://dx.doi.org/10.1016/j.cell.2005.11.011.
26. **Ojha A, Anand M, Bhatt A, Kremer L, Jacobs WR, Jr, Hatfull GF.** 2005. GroEL1: a dedicated chaperone involved in mycolic acid synthesis during biofilm formation in mycobacteria. Cell **123:**861–873. http://dx.doi.org/10.1016/j.cell.2005.09.012.
27. **Recht J, Kolter R.** 2001. Glycopeptidolipid acetylation affects sliding motility and biofilm formation in Mycobacterium smegmatis. J Bacteriol **183:**5718–5724. http://dx.doi.org/10.1128/jb.183.19.5718-5724.2001.
28. **Hall-Stoodley L, Costerton JW, Stoodley P.** 2004. Bacterial biofilms:

from the natural environment to infectious diseases. Nat Rev Microbiol **2:**95–108. http://dx.doi.org/10.1038/nrmicro821.
29. **Davey ME, O'Toole GA.** 2000. Microbial biofilms: from ecology to molecular genetics. Microbiol Mol Biol Rev **64:**847–867. http://dx.doi.org/10.1128/MMBR.64.4.847-867.2000.
30. **Watnick P, Kolter R.** 2000. Biofilm, city of microbes. J Bacteriol **182:**2675–2676. http://dx.doi.org/10.1128/JB.182.10.2675-2679.2000.
31. **Webb JS, Givskov M, Kjelleberg S.** 2003. Bacterial biofilms: prokaryotic adventures in multicellularity. Curr Opin Microbiol **6:**578–585. http://dx.doi.org/10.1016/j.mib.2003.10.014.
32. **Kreft JU.** 2004. Conflicts of interest in biofilms. Biofilms **1:**265–276. http://dx.doi.org/10.1017/S1479050504001486.
33. **Parsek MR, Fuqua C.** 2004. Biofilms 2003: emerging themes and challenges in studies of surface-associated microbial life. J Bacteriol **186:**4427–4440. http://dx.doi.org/10.1128/JB.186.14.4427-4440.2004.
34. **Battin TJ, Sloan WT, Kjelleberg S, Daims H, Head IM, Curtis TP, Eberl L.** 2007. Microbial landscapes: new paths to biofilm research. Nat Rev Microbiol **5:**76–81. http://dx.doi.org/10.1038/nrmicro1556.
35. **Hall-Stoodley L, Lappin-Scott H.** 1998. Biofilm formation by the rapidly growing mycobacterial species Mycobacterium fortuitum. FEMS Microbiol Lett **168:**77–84. http://dx.doi.org/10.1111/j.1574-6968.1998.tb13258.x.
36. **Sternberg C, Tolker-Nielsen T.** 2006. Growing and analyzing biofilms in flow cells. Curr Protoc Microbiol Chapter **1:**Unit 1B.2.
37. **Jurcisek JA, Dickson AC, Bruggeman ME.** 2011. In vitro biofilm formation in an 8-well chamber slide. J Vis Exp **47:**2481.
38. **Zou H, Koh JJ, Li J, Qiu S, Aung TT, Lin H, Lakshminarayanan R, Dai X, Tang C, Lim FH, Zhou L, Tan AL, Verma C, Tan DT, Chan HS, Saraswathi P, Cao D, Liu S, Beuerman RW.** 2013. Design and synthesis of amphiphilic xanthone-based, membrane-targeting antimicrobials with improved membrane selectivity. J Med Chem **56:**2359–2373. http://dx.doi.org/10.1021/jm301683j.
39. **National Research Council.** 2011. Guide for the care and use of laboratory animals, 8th ed. National Academies Press, Washington, DC.
40. **Crosson CE, Klyce SD, Beuerman RW.** 1986. Epithelial wound closure in the rabbit cornea. A biphasic process. Invest Ophthalmol Vis Sci **27:**464–473.
41. **Woods GL, Brown-Elliott BA, Desmond EP, Hall GS, Heifets L, Pfyffer GE, Ridderhof MR, Wallace RJ, Warren NJ, Witebsky FG.** 2003. Susceptibility testing of mycobacteria, nocardia, and other aerobic actinomycetes; approved standard. M24-A. NCCLS, Wayne, PA.
42. **Brown BA, Swenson JM, Wallace RJ, Jr.** 1994. Broth microdilution MIC test for rapidly growing mycobacteria, p 5.11.1. *In* Isenberg HD (ed), Clinical microbiology procedures handbook. American Society for Microbiology, Washington, DC.
43. **Set R, Rokade S, Agrawal S, Shastri.** 2010. Antimicrobial susceptibility testing of rapidly growing mycobacteria by microdilution—experience of a tertiary care centre. Indian J Microbiol **28:**48–50. http://dx.doi.org/10.4103/0255-0857.58729.
44. **Lee KW, Periasamy S, Mukherjee M, Xie C, Kjelleberg S, Rice SA.** 2014. Biofilm development and enhanced stress resistance of a model, mixed-species community biofilm. ISME J **8:**894–907. http://dx.doi.org/10.1038/ismej.2013.194.
45. **Ghafoor A, Hay ID, Rehm BH.** 2011. Role of exopolysaccharides in Pseudomonas aeruginosa biofilm formation and architecture. Appl Environ Microbiol **77:**5328–5346.
46. **Shi T, Fu T, Xie J.** 2011. Polyphosphate deficiency affects the sliding motility and biofilm formation of Mycobacterium smegmatis. Curr Microbiol **63:**470–476. http://dx.doi.org/10.1007/s00284-011-0004-4.
47. **Fowler AM, Dutton JJ, Fowler WC, Gilligan P.** 2008. Mycobacterium chelonae canaliculitis associated with SmartPlug use. Ophthal Plast Reconstr Surg **24:**241–243. http://dx.doi.org/10.1097/IOP.0b013e3181724302.
48. **Flemming HC, Thomas RN, Wozniak DJ.** 2007. The EPS matrix: the "house of biofilm cells." J Bacteriol **189:**7945–7947.
49. **Lewis K.** 2001. Riddle of biofilm resistance. Antimicrob Agents Chemother **45:**999–1007. http://dx.doi.org/10.1128/AAC.45.4.999-1007.2001.
50. **Xavier JB, Foster KR.** 2007. Cooperation and conflict in microbial biofilms. Proc Natl Acad Sci U S A **104:**876–881. http://dx.doi.org/10.1073/pnas.0607651104.
51. **Rose SJ, Babrak LM, Bermudez LE.** 2015. Mycobacterium avium possesses extracellular DNA that contributes to biofilm formation, structural integrity and tolerance to antibiotics. PLoS One **10**(5)**:**e0128772. http://dx.doi.org/10.1371/journal.pone.0128772.
52. **Thomas CM, Nielsen KM.** 2005. Mechanisms of, and barriers to, horizontal gene transfer between bacteria. Nat Rev Microbiol **3:**711–721. http://dx.doi.org/10.1038/nrmicro1234.
53. **Thurlow LR, Hanke ML, Fritz T, Angle A, Aldrich A, Williams SH, Engebretsen IL, Bayles KW, Horswill AR, Kielian T.** 2011. Staphylococcus aureus biofilms prevent macrophage phagocytosis and attenuate inflammation in vivo. J Immunol **186:**6585–6596. http://dx.doi.org/10.4049/jimmunol.1002794.
54. **de la Cruz J, Pineda R.** 2007. LASIK-associated atypical mycobacteria keratitis: a case report and review of the literature. Int Ophthalmol Clin **47:**73–84. http://dx.doi.org/10.1097/IIO.0b013e318037751b.
55. **Covert TC, Rodgers MR, Reyes AL, Stelma GN.** 1999. Occurence of nontuberculous mycobacteria in environ-mental samples. Appl Environ Microbiol **65:**2492–2496.
56. **Carson LA, Peterson NJ, Favero MS, Aguero SM.** 1978. Growth characteristics of atypical mycobacteria in water and their comparative resistance to disinfectants. Appl Environ Microbiol **36:**839–846.
57. **Panwalker AP, Fuhse E.** 1986. Nosocomial Mycobacterium gordonae pseudoinfection from contaminated ice machines. Infect Control **7:**67–70.
58. **Falkinham JO.** 1996. Epidemiology of infection by nontuberculous mycobacteria. Clin Microbiol Rev **9:**177–215.
59. **Bullington RH, Jr, Lanier JD, Font RL.** 1992. Nontuberculous mycobacterial keratitis. Report of two cases and review of the literature. Arch Ophthalmol **110:**519–524.
60. **Wunsh SE, Boyle GL, Leopold IH, Littman ML.** 1969. Mycobacterium fortuitum infection of corneal graft. Arch Ophthalmol **82:**602–607. http://dx.doi.org/10.1001/archopht.1969.00990020600006.
61. **Aylward GW, Stacey AR, Marsh RJ.** 1987. Mycobacterium chelonei infection of a corneal graft. Br J Ophthalmol **71:**690–693. http://dx.doi.org/10.1136/bjo.71.9.690.
62. **Eiferman RA, Stagner JI.** 1982. Intraocular penetration of amikacin. Iris binding and bioavailability. Arch Ophthalmol **100:**1817–1819.
63. **Hamam RN, Nouredin B, Salti HI, Haddad R, Khoury JM.** 2006. Recalcitrant post-LASIK Mycobacterium chelonae keratitis eradicated after the use of fourth-generation fluoroquinolone. Ophthalmology **113:**950–954. http://dx.doi.org/10.1016/j.ophtha.2006.02.028.
64. **Alexandrakis G, Alfonso EC, Miller D.** 2000. Shifting trends in bacterial keratitis in south Florida and emerging resistance to fluoroquinolones. Ophthalmology **107:**1497–1502. http://dx.doi.org/10.1016/S0161-6420(00)00179-2.
65. **de la Cruz J, Behlau I, Pineda R.** 2007. Atypical mycobacterial keratitis after laser in situ keratomileusis unresponsive to fourth-generation fluoroquinolone therapy. J Cataract Refract Surg **33:**1318–1321. http://dx.doi.org/10.1016/j.jcrs.2007.03.035.
66. **Moshirfar M, Meyer JJ, Espandar L.** 2007. Fourth generation fluoroquinolone-resistant mycobacterial keratitis after laser in situ keratomileusis. J Cataract Refract Surg **33:**1978–1981. http://dx.doi.org/10.1016/j.jcrs.2007.07.019.
67. **Steed KA, Falkinham JO, III.** 2006. Effect of growth in biofilms on chlorine susceptibility of Mycobacterium avium and Mycobacterium intracellulare. Appl Environ Microbiol **72:**4007–4011. http://dx.doi.org/10.1128/AEM.02573-05.
68. **Chambless JD, Hunt SM, Stewart PS.** 2006. A three-dimensional computer model of four hypothetical mechanisms protecting biofilms from antimicrobials. Appl Environ Microbiol **72:**2005–2013. http://dx.doi.org/10.1128/AEM.72.3.2005-2013.2006.